


The nicotinamide phosphoribosyltransferase antagonist FK866 inhibits growth of prostate tumour spheroids and increases doxorubicin retention without changes in drug transporter and cancer stem cell protein expression

Heinrich Sauer¹  | Henning Kampmann¹ | Farhad Khosravi¹ | Fatemeh Sharifpanah¹ | Maria Wartenberg²

¹Department of Physiology, Faculty of Medicine, Justus Liebig University, Gießen, Germany

²Department of Cardiology, University Heart Center, Jena University Hospital, Jena, Germany

Correspondence

Heinrich Sauer, Department of Physiology, Justus Liebig University Gießen, Aulweg 129, Gießen 35392, Germany.
Email: heinrich.sauer@physiologie.med.uni-giessen.de

Abstract

Nicotinamide phosphoribosyltransferase (NAMPT) is a rate-limiting enzyme for nicotinamide adenine dinucleotide (NAD) synthesis and is involved in cancer cell proliferation through regulation of energy production pathways. Therefore, NAMPT inhibitors are promising drugs for cancer therapy by limiting energy supply of tumours. Herein, we demonstrated that the NAMPT inhibitor FK866 ((E)-N-(4-(1-Benzoylpiperidin-4-yl)butyl)-3-(pyridin-3-yl)acrylamide) dose-dependently inhibited growth and cell motility of DU-145 prostate tumour spheroids and decreased the intracellular ATP concentration. The apoptosis marker cleaved caspase-3 remained unchanged, but the autophagy marker microtubule-associated protein 1A/1B-light chain 3 (LC3) was upregulated. Growth inhibition was reversed upon co-administration of NAD to the cell culture medium. FK866 decreased calcein as well as pheophorbide A efflux from tumour spheroids and increased doxorubicin toxicity, indicating interference with function of drug efflux transporters. DU-145 multicellular tumour spheroids expressed the stem cell associated markers CD133, CD44, Oct4, Nanog, Sox2, and drug transporters ABCB1, ABCG2, and ABCC1 which are associated with stem cell properties in cancer cells. The ABCB1 inhibitor zosuquidar, the ABCG2 inhibitor Ko143, and the ABCC1 inhibitor MK571 increased calcein retention. Neither protein expression of stem cell markers, nor drug transporters was significantly changed upon FK866 treatment. In conclusion, our data suggest that FK866 inhibits prostate cancer cell proliferation by interference with the energy metabolism, and function of drug efflux transporters.

KEYWORDS

ABCB1, ABCC1, ABCG2, autophagy, cancer stem cells, multidrug resistance, nicotinamide phosphoribosyltransferase, prostate tumour spheroid

[Correction added on 6 January, after first online publication: The third author's last name has been corrected.]

This is an open access article under the terms of the Creative Commons Attribution-NonCommercial License, which permits use, distribution and reproduction in any medium, provided the original work is properly cited and is not used for commercial purposes.

© 2020 The Authors. Clinical and Experimental Pharmacology and Physiology published by John Wiley & Sons Australia, Ltd

1 | INTRODUCTION

Cancer cells are rapidly dividing cells, thus having a high energy demand, which has to be fulfilled even in the hypoxic conditions in the depth of solid tumours. The dysregulated tumour metabolism is shifted from energy generation in the tricarboxylic acid (Krebs) cycle to glycolysis (Warburg effect) to maintain robust and rapid cancer cell proliferation.^{1,2} This specificity of cancer cell metabolism has raised the idea to specifically interfere with cancer-associated metabolic pathways in order to fight cancer by energy deprivation of cancer cells. Energy-demanding metabolic pathways require metabolites, such as the co-enzyme NAD. NAD plays a central role in various cellular redox reactions and several cell survival- and proliferation-supporting functions, such as regulation of mitochondrial function, and stimulation of glycolysis via glyceraldehyde 3-phosphate dehydrogenase (GAPDH) and lactate dehydrogenase.³ NAD is regulating serine biosynthesis in tumour cells, and is a substrate for poly(ADP-ribose)polymerase (PARP), a major player in DNA repair processes. Moreover, NAD is required for the function of sirtuins, which consume NAD to control cell longevity and cell survival under stress conditions.⁴ In mammalian cells, NAD generation is mainly regulated by the salvage pathway, which involves two central enzymes, ie nicotinamide mononucleotide adenylyltransferase (NMNAT) and nicotinamide phosphoribosyltransferase (NAMPT), which is the rate-limiting enzyme in this pathway and converts nicotinamide (NAM) to nicotinamide mononucleotide (NMN). Subsequently, NMNAT generates NAD by transferring the adenylyl moiety from ATP to NMN. Alternatively, NAD can be synthesized de novo from tryptophan, which occurs predominantly in the liver or in the *Preiss-Handler* (PH) pathway, where nicotinate phosphoribosyltransferase (NAPRT) catalyzes the synthesis of nicotinic acid mononucleotide (NAMN) from nicotinic acid (NA) and 5-phosphoribose-1-pyrophosphate (PRPP). NMNAT is then conjugating ATP to NAMN to generate NAD.⁵ In the past years, an increasing number of pharmacologic inhibitors of NAMPT has been developed to deprive cancer cells from NAD and consequently energy supply. Since non-cancerous cells are able to use any of the NAD-generating biochemical pathways, they do not die in response to NAMPT inhibitors like FK866, or si-RNA-mediated down-regulation of enzymes involved in de novo NAD synthesis, the PH pathway or salvage pathways.⁶ This observation underscores the possibility to target specifically cancer cells through NAMPT inhibition and relieve non-cancerous cells under these conditions. Overexpression of NAMPT has been observed in a variety of tumours including prostate cancer.⁷ The increased NAD concentrations in NAMPT-overexpressing cancer cells are supporting rapid cycling times of cancer cells and increase cancer cell survival in presence of anticancer agents.⁸ Although NAMPT inhibitors are promising candidates for preventing tumour cell growth, clinical studies using FK866 displayed toxicity to normal, rapidly proliferating hematopoietic cells, and had to be discontinued, due to side effects like thrombocytopenia.⁹ This observation prompted the development of a new generation of NAMPT inhibitors with less toxicity, which may be used in therapeutic partnership with PARP inhibitors¹⁰

According to the cancer stem cell (CSC) hypothesis, a tiny group of stem cell-like cells are responsible for development and progression of cancer disease. Cancer stem cells are highly proliferative and contribute to tumour growth and spread of tumours within the body.^{11,12} Notably, expression of stem cell markers is frequently associated with transporters of the ABC (ATP binding cassette) family. Therefore, upon emergence of drug resistance due to overexpression of drug transporters, chemo/radiation therapy fails to eradicate CSCs, thereby leading to CSC-mediated clinical relapse.¹³ Moreover, it has been shown that occurrence of drug resistance as well as stem cell gene expression is strikingly dependent on the tumour micro-environment and three-dimensional (3D) structure of the tumour. In this respect, it has been shown that chemo/radiation resistance of tumour cells is increased when cells are grown as spherical tumour spheroids in comparison to two-dimensional cell cultures.^{14,15} Chemo/radiation resistance is enhanced in the hypoxic tumour tissue milieu, which regulates both expression of drug transporters like ABCB1,¹⁵ ABCG2,¹⁶ ABCC1¹⁷ and pluripotency-determining stem cell genes¹⁸

In the present study, we cultivated DU-145 prostate cancer cells as 3D multicellular tumour spheroids and investigated tumour growth, tumour cell motility, ATP content, doxorubicin toxicity, and protein expression of stem cell genes and the drug transporters ABCB1, ABCG2, and ABCC1 upon treatment with different concentrations of the NAMPT inhibitor FK866. Our data demonstrated that interference with NAMPT results in growth inhibition, as well as increased drug retention of tumour spheroids, which suggests inhibition of drug transporter function presumably by ATP deprivation. Notably, protein expression of stem cell genes and drug transporters was not changed upon NAMPT inhibition indicating that their expression does not rely on intracellular NAD concentrations.

2 | RESULTS

2.1 | Effect of NAMPT inhibition on tumour spheroid growth and cell motility

To investigate the cytotoxicity of the NAMPT inhibitor FK866, 10-day-old tumour spheroids with diameters approximating $120 \pm 17 \mu\text{m}$ were incubated with different concentration of this compound, ranging from 5 to 40 nmol/L, and tumour spheroid growth was monitored during subsequent 5 days (day 10–day 15 of cell culture). It was evident that FK866 dose-dependently inhibited the growth of tumour spheroids (Figure 1) ($n = 3$). To investigate the toxicity of FK866 in more detail, tumour spheroids were double-labelled with SYTOX green, which intercalates in the DNA of cells with compromised cell membranes, and DRAQ5, which is permeable in living and dead cells. Our data clearly showed, that following 5 days of treatment, the number of dead cells increased with enhanced FK866 concentration (Figure 2) ($n = 3$). Moreover, detached cells from FK866-treated tumour spheroids were not vital as indicated by Sytox green/DRAQ5 double staining (data not shown). Besides inhibition

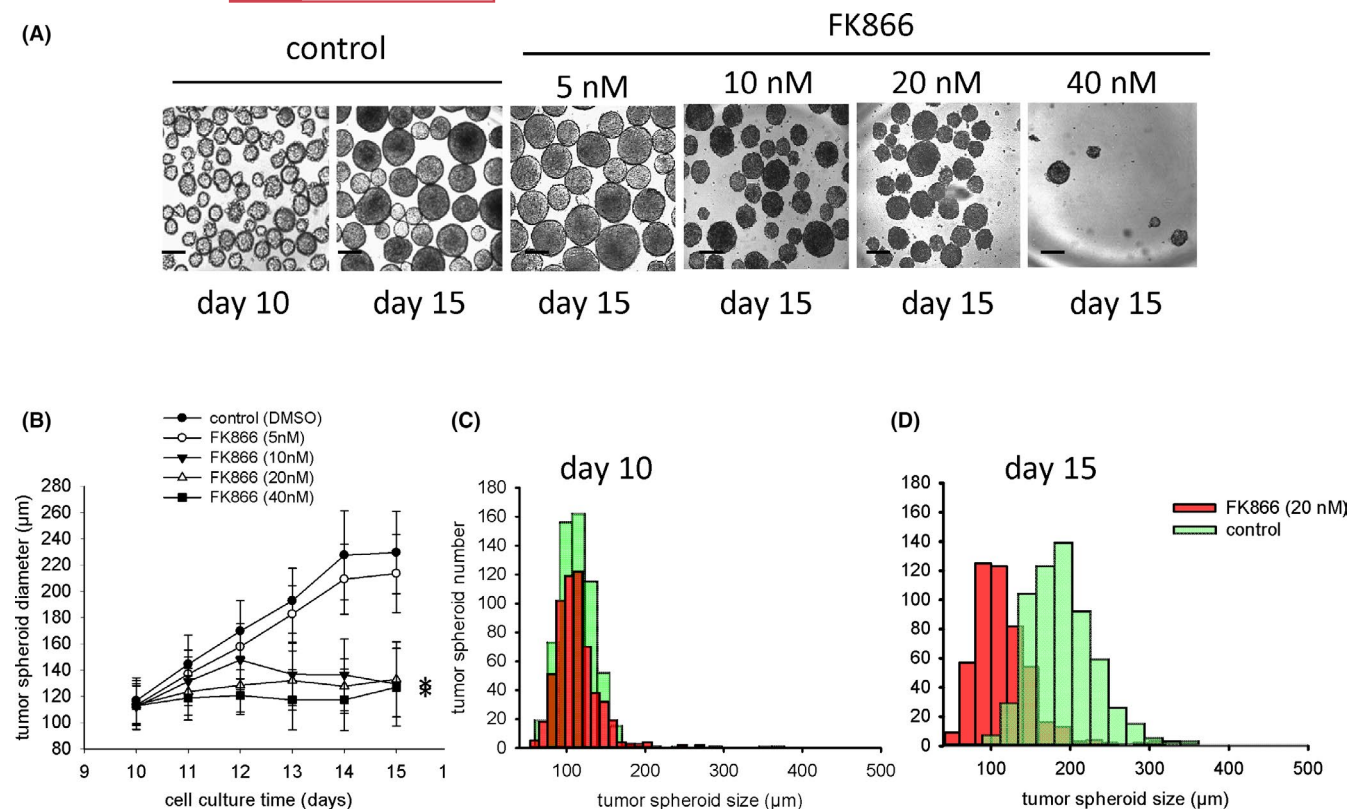


FIGURE 1 Effect of different concentrations of FK866 on the growth of multicellular DU-145 tumour spheroids. Tumour spheroids were treated from day 10 to day 15 of cell culture. The DMSO sample was used as vehicle control. (A) Representative transmission images of tumour spheroids. The bar represents 200 μm. (B) Line and scatter plot of tumour spheroid growth over time (n = 3). (C, D) Histogram of size distribution of tumour spheroids before treatment (day 10), and after 5 d of treatment with FK866 (20 nM). * $P \leq .05$, significantly different to the vehicle control

of tumour spheroid growth, inhibition of NAMPT by FK866 may interfere with tumour cell motility. To investigate this issue, tumour spheroids were outgrown and their outgrowth area was determined as indicator of cell motility. As shown in Figure 3A, FK866 dose-dependently decreased the outgrowth of cells from DU-145 tumour spheroids, indicating inhibition of cell motility. The outgrowth inhibition effect upon incubation with 10 nmol/L FK866 was abolished upon co-administration of extracellular NAD (10 μmol/L), indicating that the observed effect was due to NAD-deprivation in the tumour cells rather than an off-target non-specific effect of the compound (Figure 3B) (n = 3). To assess the mechanism of tumour cell death, apoptosis was investigated in tumour spheroids. To achieve this aim, tumour spheroids were treated with either 5 or 20 nM FK866 for 5 days and the apoptosis marker cleaved caspase-3 was assessed (Figure 4A, n = 4). Our data demonstrated that FK866 treatment slightly, but not significantly increased the ratio of pro-caspase 3 to cleaved caspase 3 expression. However, when single tumour cells were treated with 20 nM FK866 and stained against the autophagy marker LC3, a significant increase in LC3-I expression was observed in immunohistochemistry experiments (Figure 4B, n = 5), indicating initiation of autophagic processes. These data were confirmed by western blot analysis (Figure 4C, n = 3), which demonstrated that treatment with 5 and 20 nM FK866 significantly increased LC3-I expression, whereas LC3-II expression remained unchanged.

2.2 | FK866 increases doxorubicin toxicity in DU-145 tumour spheroids

Cytostatic anthracyclines are generally used in clinical therapy to treat multiple types of cancer. It is a first-line chemotherapy treatment for patients with metastasized, hormone-resistant prostate cancer (PCa) or for patients with high-risk, localized PCa that could benefit from early chemotherapy treatment.¹⁹ Generally, chemotherapy is associated with severe side effects, which increase with the dose of the applied chemotherapeutic. One measure to avoid side effects of chemotherapy would therefore be the combination of two or more substances at low concentrations to achieve an additive cytotoxic effect. To test this aspect, we investigated the dose-dependent toxicity of doxorubicin in DU-145 prostate cancer cells. Our data demonstrated that doxorubicin dose-dependently decreased the outgrowth/tumour spheroid diameter ratio in a concentration range between 0.1 and 5 μmol/L, when applied over a time period of 5 days (Figure 5A, n = 2). In a next step we incubated outgrown tumour spheroids for 5 days with 0.1 μmol/L doxorubicin either in presence or absence of 10 nmol/L FK866. Our data indicate, that the cytotoxic effect of doxorubicin was increased in presence of FK866 (10 nmol/L), indicating that this compound may be used as adjuvant in anthracycline cancer treatment (Figure 5B, n = 5).

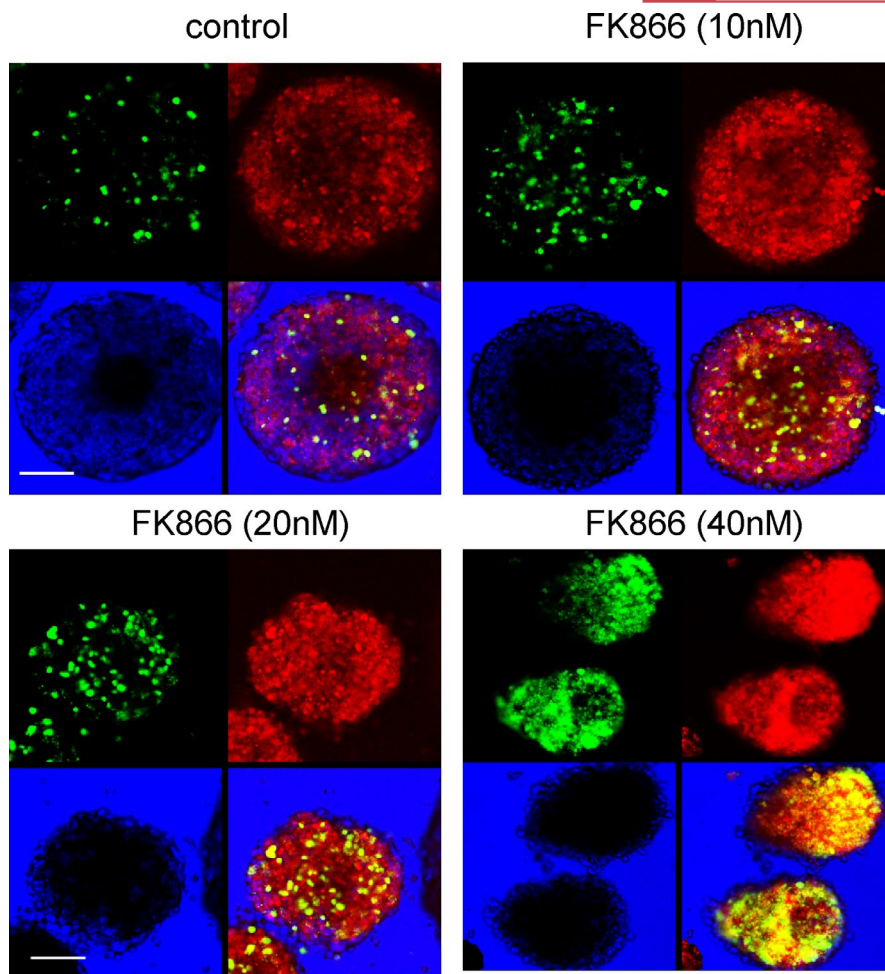


FIGURE 2 Toxicity of different FK866 concentrations in DU-145 tumour spheroids. Tumour spheroids were treated from day 10 to day 15 of cell culture with either 10, 20 or 40 nmol/L FK866, and cell vitality was assessed by double labelling with the dead cell indicator Sytox green, and the live and dead cell indicator DRAQ5. It was evident that FK866 treatment dose-dependently increased the number of Sytox green-positive cells ($n = 3$). Green: Sytox green, red: DRAQ5, blue: transmission, green/red/blue: overlay image. The bar represents 50 μm

2.3 | FK866 increases calcein and doxorubicin retention in DU-145 tumour spheroids, but decreases intracellular ATP

We and others have previously shown that DU-145 multicellular tumour spheroids develop an intrinsic drug resistance, which is dependent on the three-dimensional tissue context and regulated by hypoxia-inducible factor-1 α (HIF-1 α) in the hypoxic milieu of the tumour tissue.^{15,20} We therefore investigated, whether FK866 would interfere with drug efflux from tumour spheroids, and loaded tumour spheroids (10-day-old) with the live cell indicator and drug transporter substrate calcein AM (0.1 $\mu\text{mol/L}$)²¹ either in absence or presence of FK866 (40 nmol/L), which was pre-incubated for 24 hours. In parallel, efflux of pheophorbide A (5 $\mu\text{mol/L}$), which is a substrate for ABCG2,²² was assessed in absence and presence of FK866. After loading with calcein AM, tumour spheroids were washed and calcein retention was monitored over 180 minutes. It was evident that pre-treatment with FK866 significantly increased calcein retention in multicellular tumour spheroids, which was

significant after 120 and 180 minutes, thus indicating that FK866 was interfering with drug efflux mechanisms (Figure 6A,B, $n = 4$). Moreover, FK866 totally abolished pheophorbide A efflux from tumour spheroids (Figure 6C, $n = 3$). When tumour spheroids were co-labelled with calcein and doxorubicin (0.1 $\mu\text{mol/L}$), calcein as well as doxorubicin fluorescence was significantly increased upon pre-incubation with FK866 (Figure 6D,E, $n = 3$), thus corroborating our experiments on increased doxorubicin toxicity in presence of FK866, and suggesting that the efflux of calcein and doxorubicin was inhibited under these experimental conditions. This assumption was validated by experiments where tumour spheroids were pre-incubated for 24 hours with FK866, and for 2 hours with the ABCB1 antagonist zosuquidar (0.1 $\mu\text{mol/L}$), the ABCG2 antagonist Ko143 (0.1 μM), or the ABCC1 inhibitor MK-571 (50 $\mu\text{mol/L}$). All antagonists of drug extrusion transporters elevated calcein retention (Figure 6F, $n = 3$). Co-administration of FK866 with either Ko143, zosuquidar, or MK-571 did not significantly increase calcein retention. Taken together these data suggest that ABCB1, ABCG2, and ABCC1 are contributing to the drug efflux mechanism in DU-145 tumour spheroids.

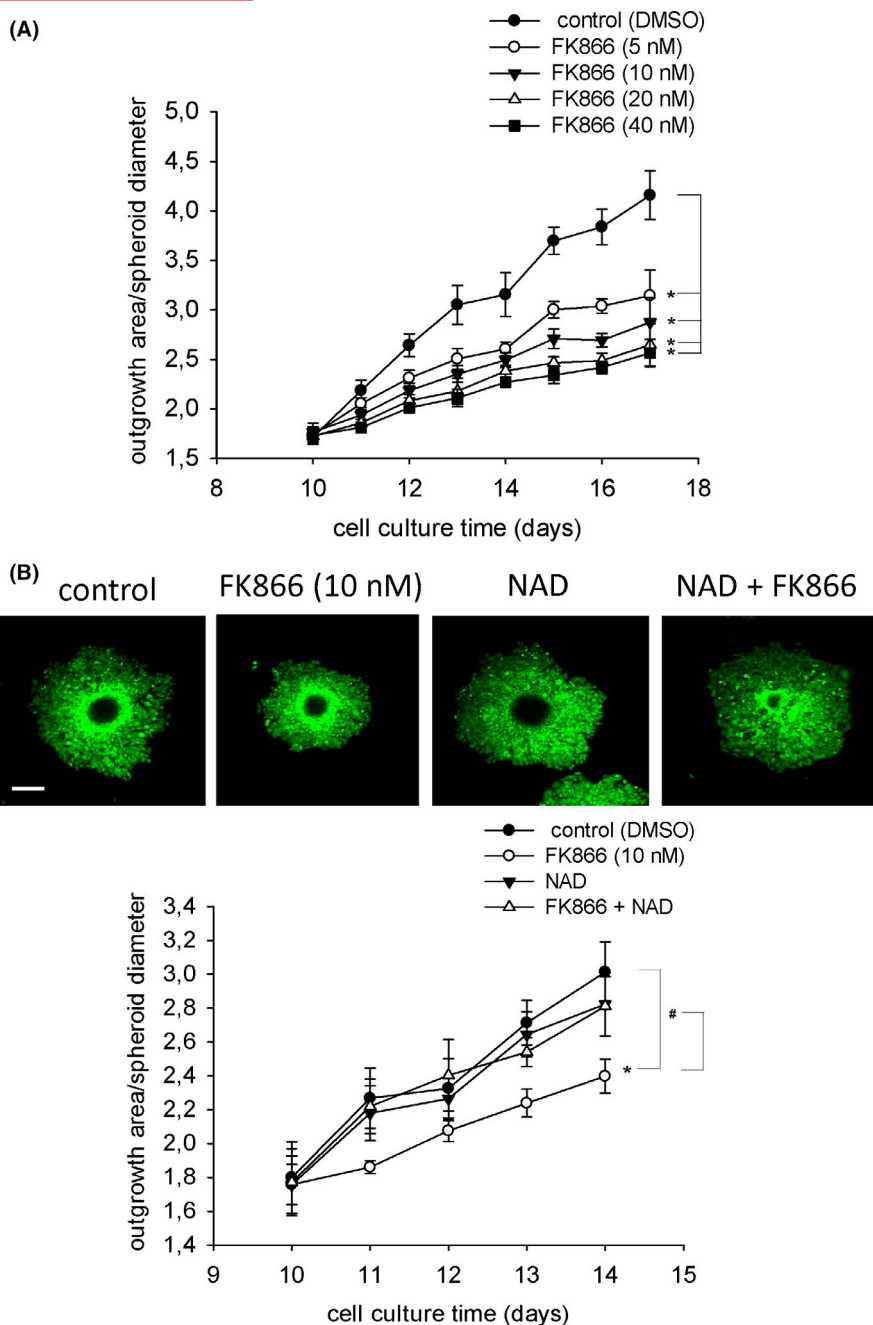


FIGURE 3 Outgrowth of DU-145 multicellular tumour spheroids following treatment with different concentrations of FK866. Tumour spheroids were plated on day 10 of cell culture to coverslips, and the ratio between outgrowth area and tumour spheroid diameter was assessed after staining with the live cell indicator calcein AM. (A) Effect of different doses of FK866 on tumour cell outgrowth from tumour spheroids ($n = 3$). (B) Reversal of outgrowth inhibition upon FK866 (10 nmol/L) by exogenous NAD (10 μ mol/L) ($n = 3$). The upper panel in (B) shows representative calcein-labelled outgrown tumour spheroids. The bar represents 100 μ m. * $P \leq .05$, significantly different to the vehicle control. # $P \leq .05$, significantly different to the FK866 treated sample

Since ABC transporters are primary active, thus needing ATP for proper transport function, intracellular ATP concentrations were determined. It was shown that treatment of tumour spheroids for 48 hours with either 20 or 40 nmol/L FK866, decreased the intracellular ATP content by approximately 35% (Figure 7, $n = 4$), which represents a significant linear trend and suggests that the observed reduction in drug efflux may be due to limited ATP availability for drug transporters.

2.4 | Protein expression of stem cell markers, as well as the drug efflux transporters ABCB1, ABCG2, and ABCC1

The efficiency of cancer chemotherapy is hampered by intrinsic and acquired drug resistance, and presence of drug resistant CSCs. Prostate cancer cells, including cells from the DU-145 cell line, have been previously demonstrated to express stem cell markers when

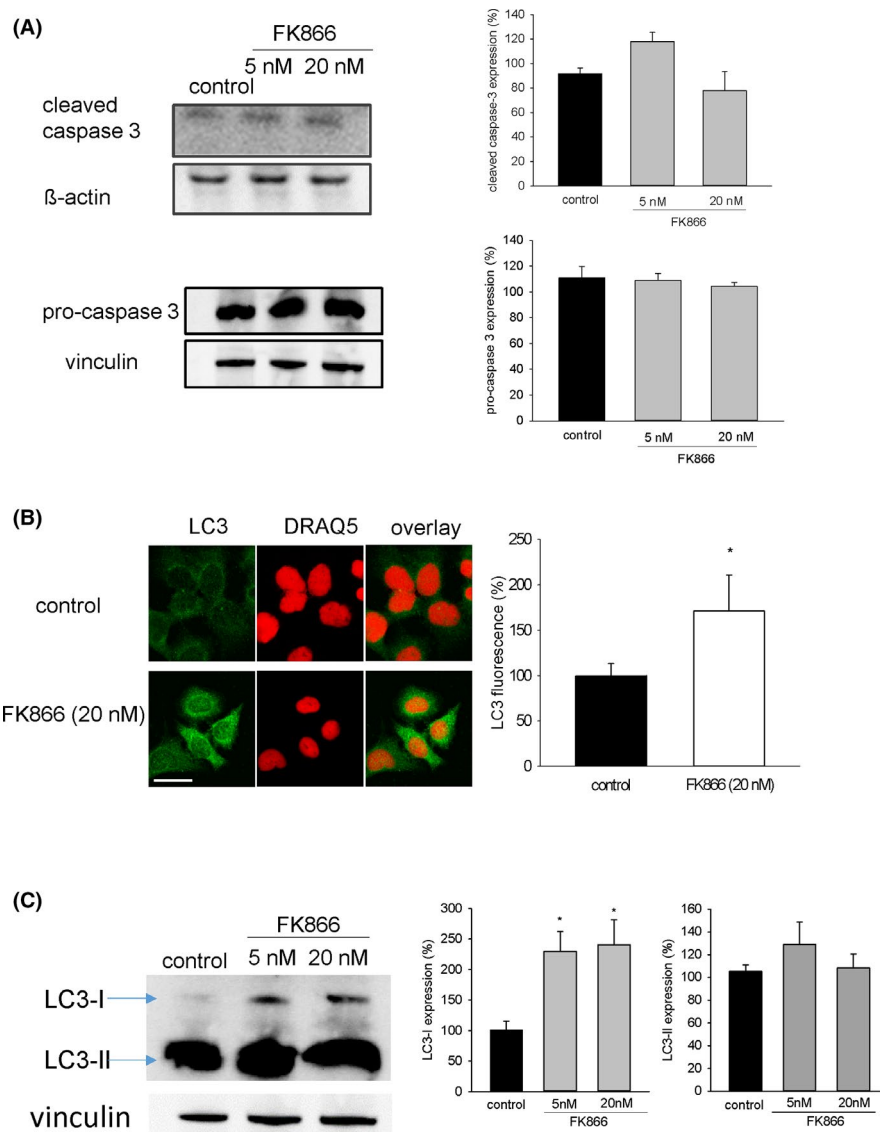


FIGURE 4 Effect of FK866 on apoptosis and autophagy in DU-145 tumour cells. (A) Protein expression of the apoptosis marker cleaved caspase 3 and pro-caspase 3 in DU-145 tumour spheroids treated from day 10 to day 15 of cell culture with either 5 or 20 nmol/L FK866. β -actin, as well as vinculin were used as loading control. Shown is a representative western blot. The bar chart shows the mean \pm SEM of $n = 4$ independent experiments. (B) LC3 expression in single cells DU-145 tumour cells which were treated for 48 h with FK866 (20 nmol/L). Shown are representative cells, which were labelled with an antibody directed against LC3 (green), and with the nuclear marker DRAQ5 (red) presented either separately or in overlay images. The bar represents 35 μ m. The bar chart shows the mean \pm SEM of five independent experiments. (C) Protein expression of LC3-I and LC3-II. Shown is a representative western blot. Vinculin was used as loading control. The bar charts show the means \pm SEM of three independent experiments. * $P \leq .05$, significantly different to the vehicle control

cultured as prostaspheres.²³ Stem cell properties are frequently associated with expression of the drug extrusion transporters ABCB1 and ABCG2, which are regulated by hypoxia.^{15,18} We therefore investigated whether inhibition of NAD generation by FK866 would affect protein expression of the stem cell proteins CD44, CD133, Nanog, Oct4, Sox2, and ABCB1, ABCG2, ABCC1. Our data showed that incubation for 5 days with 5 and 20 nmol/L FK866 did not significantly change expression of stem cell proteins (Figure 8A–E, $n = 4$), and drug extrusion transporters ABCB1 (Figure 8F, $n = 4$), ABCG2 (Figure 8G, $n = 4$), and ABCC1 (Figure 8H, $n = 3$). This suggests, that the observed increased calcein retention in DU-145 tumour

spheroids was not due to decreased expression of drug extrusion transporters, and expression of stem cell markers did not protect DU-145 tumour cells from the cytotoxic action of FK866.

3 | DISCUSSION

Targeting the metabolism of tumour cells is a promising strategy to fight cancer. This may be achieved by NAMPT inhibition, which leads to attenuation of glycolysis at the glyceraldehyde 3-phosphate dehydrogenase step due to the reduced availability of NAD

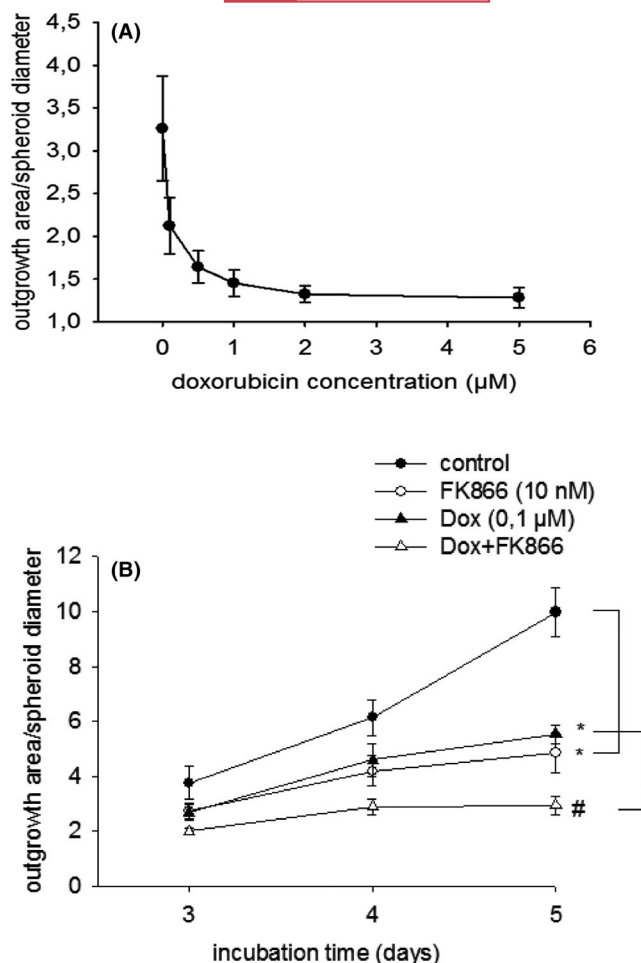


FIGURE 5 Outgrowth of DU-145 multicellular tumour spheroids following treatment with different concentrations of doxorubicin, and additive effects of doxorubicin and FK866 co-administration. (A) Plated DU-145 tumour spheroids were remained untreated or were treated with either 0.1 $\mu\text{mol/L}$, 0.5 $\mu\text{mol/L}$, 1 $\mu\text{mol/L}$, 2 $\mu\text{mol/L}$ or 5 $\mu\text{mol/L}$ doxorubicin, and the ratio between outgrowth area and tumour spheroid diameter was assessed ($n = 2$). (B) Plated tumour spheroids were either treated with doxorubicin (0.1 $\mu\text{mol/L}$), FK866 (10 nmol/L) or a combination of both ($n = 5$). Notably, FK866 treatment increased the toxicity of doxorubicin. * $P \leq .05$, significantly different to the vehicle control. # $P \leq .05$, significantly different to the doxorubicin-treated sample

for the enzyme.²⁴ The data of the present study demonstrated, that lowering intracellular NAD levels by use of the NAMPT inhibitor FK866 efficiently kills DU-145 tumour cells grown in the three-dimensional context of multicellular tumour spheroids. Growth of multicellular tumour spheroids and motility of tumour cells was inhibited even in nanomolar concentrations of FK866 (10–40 nmol/L), which was attenuated in the presence of NAD, indicating that the effect was due to limitation of NAD supply. FK866 treatment only moderately increased apoptosis, but stimulated autophagy as indicated by increased expression of LC3. It has been previously shown, that autophagic induction by starvation and energy deprivation stimulates the conversion of LC3-I to

LC3-II and upregulates LC3 expression.²⁵ Depletion of intracellular NAD levels by FK866 has been recently shown to result in autophagic death of multiple myeloma cells²⁶ as well as of adult T-cell leukaemia/lymphoma (ATL) cells.²⁷ Moreover, our data showed that FK866 increased the tissue accumulation and toxicity of doxorubicin at low dose, which may allow the clinical use of lower concentrations of this anthracycline when co-administrated with NAMPT inhibitors, thus potentially reducing the severe toxic side effects of anticancer agents especially on the heart.²⁸ DU-145 cancer cells express the drug extrusion transporters ABCB1,²⁹ ABCG2,¹⁸ and ABCC1³⁰ which are regulated by hypoxia and confer an intrinsic drug resistance, when cells are grown as hypoxic tumour spheroids. Notably, our previous data demonstrated that ABCB1 expression was upregulated by the glycolysis end-product pyruvate, suggesting that drug resistance is related to the glycolytic metabolism of tumour cells.²⁹ To evaluate the basis for increased doxorubicin toxicity upon FK866 treatment, calcein and pheophorbide A retention assays were performed. Calcein AM is a live cell stain, readily taken up by cells and cleaved by intracellular esterases to generate fluorescent calcein, which is a substrate for ABCB1 and ABCC1.³¹ Pheophorbide A is a fluorescent product of chlorophyll breakdown and specific substrate for ABCG2.³² Our data showed, that FK866 significantly inhibited calcein efflux comparably to the ABCB1 antagonist zosuquidar or the ABCG2 antagonist Ko143, suggesting that ABCB1 and ABCG2 substantially contribute to the drug resistance phenotype of DU-145 prostate tumour spheroids. Moreover, pheophorbide A efflux was inhibited by FK866, underlining the contribution of ABCG2. Since MK-571 increased calcein retention a role of ABCC1 in intrinsic drug resistance of DU-145 tumour spheroids is suggested. ABC transporters are ATPases that transport their substrates against the concentration gradient by binding and hydrolysis of ATP at the ABC moiety of the molecule.³³ In our experiments, treatment with FK866 decreased intracellular ATP, which may affect ABC transporter function. Depletion of ATP by FK866 has been previously demonstrated in breast cancer cells,³⁴ ovarian carcinoma cells³⁵ and colonic cancer cells.³⁶ Alternatively, FK866 could bind to ABC transporters and block the transport function by reducing ATPase activity. Notably, protein expression of ABCB1, ABCG2, and ABCC1 was not affected upon pre-incubation with FK866, indicating that the increased calcein retention was due to inhibition of drug transporter function, rather than protein expression. This observation is reasonable, since drug extrusion by ABC transporters requires sufficient ATP supply, which is hampered if metabolic ATP-generating pathways like glycolysis and the mitochondrial respiratory chain are running short of NAD and NADH upon NAMPT inhibition.

Expression of ABC transporters is frequently associated to stem cell features in tumour cells. Moreover, it was evidenced, that NAMPT overexpression induces pluripotency through signalling pathways, which are controlling stemness.^{37,38} Indeed, our data showed that DU-145 multicellular tumour spheroids strongly

expressed the cancer stem cell markers CD44, CD133, and the general pluripotency markers Nanog, Oct 4, and Sox2. Drug resistance is a general feature of stem cells including cancer stem cells (CSCs), which helps them to escape from anticancer therapies.

Consequently, down-regulation or inhibition of drug extrusion transporters was demonstrated to sensitize tumours towards chemotherapeutic agents via targeting CSCs.³⁹⁻⁴² Moreover, a recent study demonstrated, that either shRNA gene inactivation

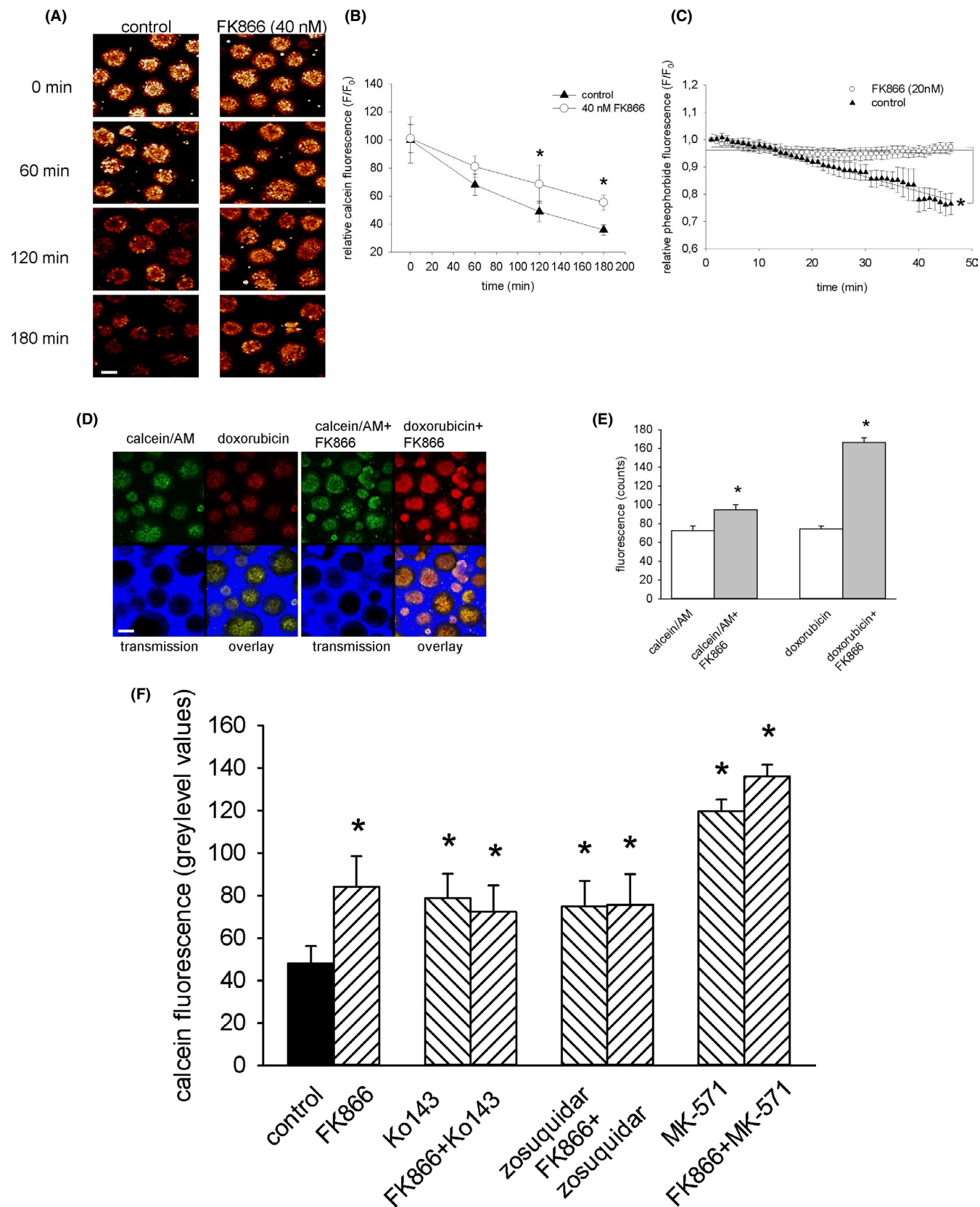


FIGURE 6 Drug retention in DU-145 tumour spheroids upon pre-incubation with FK866. Tumour spheroids (10-day-old) were incubated with FK866 (40 nmol/L) for 24 h and subsequently labelled for 30 min with either calcein AM (0.1 μ M), or for 60 min with pheophorbide A (5 μ mol/L). After washing with fresh cell culture medium, calcein fluorescence was assessed after 60, 120, and 180 min. (A) Representative calcein-labelled tumour spheroids after different times of calcein washout from the incubation medium. The bar represents 100 μ m. (B) Line and scatter plot of calcein retention in tumour spheroids after different times of calcein washout ($n = 4$). (C) Efflux kinetics of pheophorbide A, which was recorded in 60 s intervals ($n = 3$). (D, E) Effect of FK866 (40 nmol/L) on calcein and doxorubicin retention in tumour spheroids. Tumour spheroids were pre-incubated for 24 h with FK866 and 4 h before inspection with calcein AM (0.1 μ mol/L), and doxorubicin (0.1 μ mol/L). 120 min before fluorescence recording the fluorescence dyes were removed from the incubation medium. (D) Shown are representative fluorescence images of calcein (green) and doxorubicin (red) stainings, as well as overlay images. The bar represents 100 μ m. (E) The bar chart shows the mean \pm SEM of three independent experiments. (F) Effect of FK866 (40 nmol/L), the ABCB1 antagonist zosuquidar (0.1 μ mol/L), the ABCG2 antagonist Ko143 (0.1 μ mol/L) and the ABCC1 antagonist MK-571 (50 μ mol/L) on calcein retention after 180 min of calcein washout. Tumour spheroids were treated for 24 h with FK866, and for 2 h with zosuquidar, Ko143 or MK-571 either alone, or in combination with FK866 before calcein labelling ($n = 3$). * $P \leq .05$, significantly different to the vehicle control

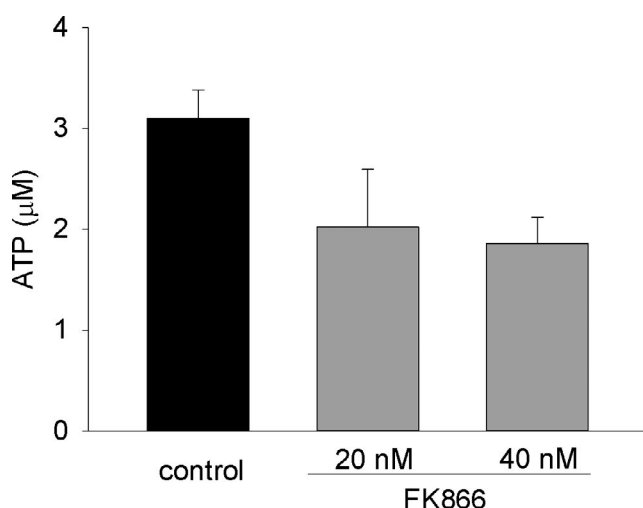


FIGURE 7 ATP concentration in tumour spheroids upon incubation with FK866. 10-day-old tumour spheroids were treated for 48 h with either 20, or 40 nmol/L FK866, and intracellular ATP concentration was determined by a fluorometric ATP assay kit. Presented are the means \pm SEM of $n = 4$ independent experiments, which showed a significant linear trend

of NAMPT or treatment with FK866 reduced the vitality of murine P19 teratocarcinoma-derived CSCs grown as single cells, and decreased the expression of pluripotency genes.⁴³ The data of the present study demonstrated that prolonged incubation with FK866 neither changed the expression of ABC transporters, nor of stem cell markers. Hence, our data suggest that the stem cell features of DU-145 multicellular tumour spheroids did not protect the cells from the toxic action of NAMPT inhibitor.

It has been recently shown that several cancers and cancer cell lines including the androgen-insensitive PC3 prostate cancer cell line lack NAPRT expression,⁴⁴ implicating that NAD synthesis in these cancer cells exclusively depends on NAMPT, and suggesting that the efficacy of FK866 treatment should be higher as compared to cancer cells that express NAPRT.⁸ Yet a recent study demonstrated that while NA did not protect NAPRT1-deficient tumour cell lines from NAMPT inhibition in vitro, it reduced efficacy of NAMPT inhibitors in cell culture- and patient-derived tumour xenografts in vivo,

presumably due to increased circulating levels of metabolites generated by mouse liver, in response to NA or through competitive reactivation of NAMPT by NAM.⁴⁵ An alternative, clinically applicable strategy could be the co-administration of DNA-damaging anticancer drugs with NAMPT inhibitors, since PARP-mediated poly ADP-ribosylation requires large amounts of NAD. Thus, in the absence of NAD, DNA repair by PARP will be impaired, and cancer cell lethality upon NAMPT inhibition be increased. Consequently, the inhibition of drug transporter function by FK866 reported in the present study will facilitate uptake of DNA-damaging agents like doxorubicin and render chemotherapy of cancer more efficient.

4 | MATERIALS AND METHODS

4.1 | Culture technique of DU-145 prostate tumour cells

The human prostate cancer cell line DU-145 was grown routinely in 5% CO₂/humidified air at 37°C with Ham's F10 medium (Gibco, Thermo Fisher Scientific) supplemented with 10% fetal bovine serum (FBS) (Gibco), 2 mmol/L L-glutamine, 0.1 mmol/L 2-mercaptoethanol, 2 mmol/L non-essential amino acids (NEA), 100 U/mL penicillin, and 50 μ g/mL streptomycin. Spheroids were grown from single cells.

4.2 | Cultivation technique of 3D multicellular tumour spheroids

Confluent cell monolayers were enzymatically dissociated with 0.1% trypsin and 0.05% EDTA (Gibco), seeded in siliconated 250 mL bioreactor flasks (Integra Biosciences) with 250 mL complete medium, and agitated at 20 strokes/min using a Cellspin stirrer system (Integra Biosciences). Cell culture medium was partially (100 mL) changed every day. For incubation with FK866, multicellular tumour spheroids (diameter 120 ± 17 μ m) were transferred to bacteriological tissue culture plates (diameter 6 cm) filled with 5 mL Ham's F10 cell culture medium. They were subsequently treated for 5 days with different concentrations of FK866 (Sigma) as indicated.

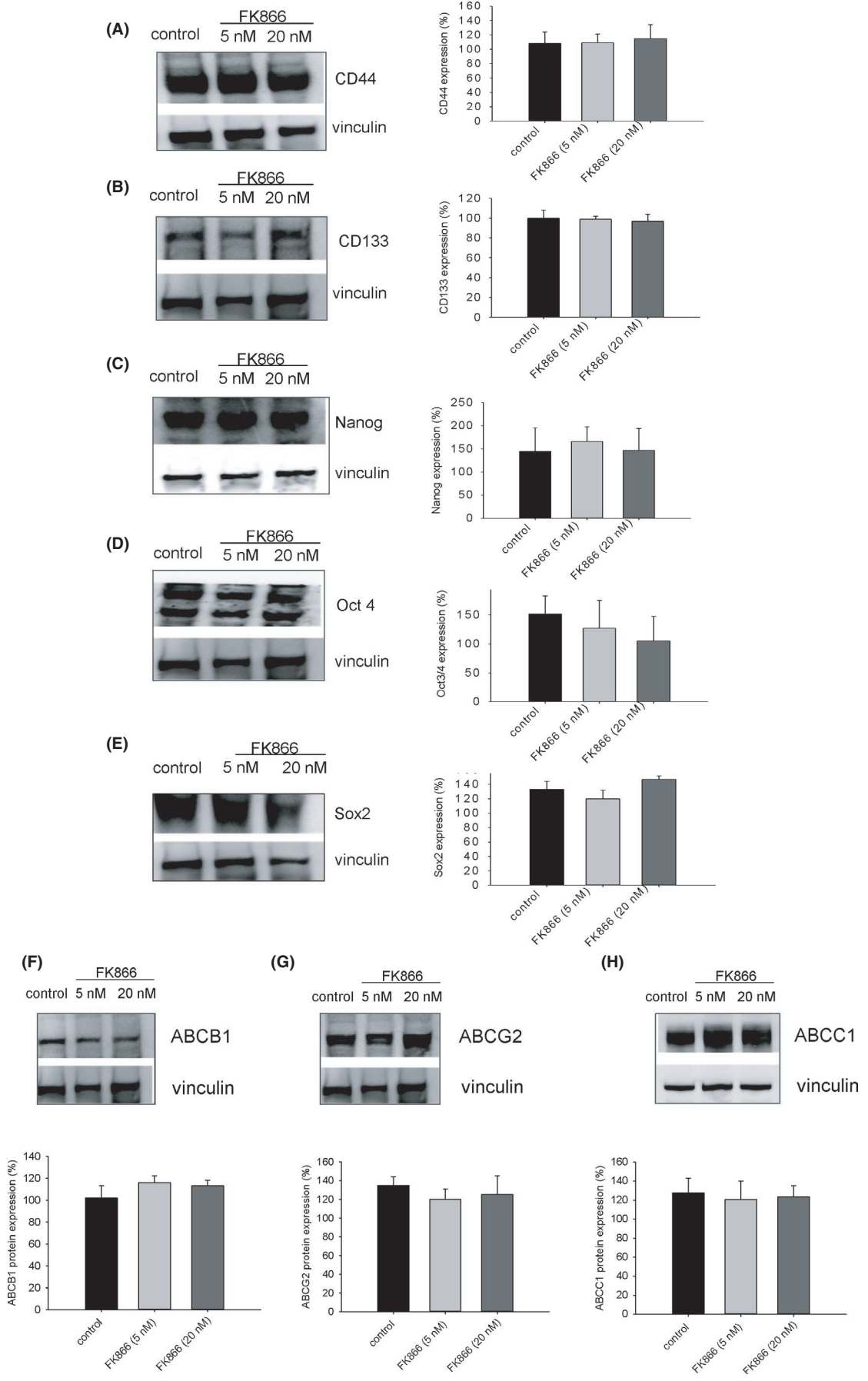


FIGURE 8 Protein expression of the stem cell genes (A) CD44, (B) CD133, (C) Nanog, (D) Oct 4 and (E) Sox 2 and the ABC transporters ABCB1 (F), ABCG2 (G), and ABCC1 (H) upon treatment of 10-day-old tumour spheroids for 5 consecutive days with either 5 or 20 nmol/L FK866. Shown are representative western blots. Vinculin was used as loading control. The bar charts show the means \pm SEM of $n = 4$ independent experiments for CD44, CD133, Nanog, Oct 4, Sox 2, ABCB1, ABCG2, and $n = 3$ for ABCC1

4.3 | Western blot analysis

Whole protein extraction was carried out after washing the tumour spheroids in PBS and lysing in RIPA lysis buffer (50 mmol/L Tris-HCl (pH 7.5), 150 mmol/L NaCl, 1 mmol/L EDTA (pH 8.0), 1 mmol/L glycerophosphate, 0.1% SDS, 1% Nonidet P-40), supplemented with protease inhibitor cocktail (Biovision) for 20 minutes on ice. Samples were centrifuged at 24 700 g for 10 minutes at 4°C to pellet the debris. After determination of the protein concentration using a Lowry protein assay, 20 μ g of protein samples were boiled for 10 minutes at 70°C, separated in PAGE Ex Precast gels (4%–12%) (Lonza), and transferred to PVDF membranes by the XCell SureLock Mini-Cell Blot Module (Invitrogen) at 180 mA for 90 minutes. Membranes were blocked with 5% (wt/vol) dry fat-free milk powder in Tris-buffered saline with 0.1% Tween (TBST) for 60 minutes at room temperature. Incubation with primary antibody was performed at 4°C overnight. Used primary antibodies were: rat anti-human ABCG2 (dilution 1:1000) (Abcam, Cat. No. ab24115), mouse anti-human ABCB1 (dilution 1:1000) (Abcam, Cat. No. ab3364), mouse anti-human ABCC1 (dilution 1:5000) (Proteintech Cat. No. 67228-1-Ig), mouse anti-human Oct4 (dilution 1:1000) (Thermo Fisher Scientific, Waltham, MA, USA, Cat. No. Mab4305MI), goat anti-human Nanog (dilution 1:1000) (Abcam, Cat. No. ab77095), rabbit anti-human CD133 (dilution 1:1000) (Abcam, Cat. No. ab16518), mouse anti-human CD44 (dilution 1:1000) (Thermo Fisher Scientific, Cat. No. PIMA515462), polyclonal rabbit anti-human Sox2 (dilution 1:1000) (Thermo Fisher Scientific, Cat. No. PA1-16968), monoclonal rabbit anti-human cleaved caspase 3 (Asp 175) (dilution 1:1000) (Cell Signaling Technology, Frankfurt, Germany, Cat. No. mAb #9664), monoclonal rabbit anti-human caspase-3 (Abcam Cat. No. ab184787), polyclonal rabbit anti-human LC3 (Proteintech, Cat. No. 14600-1-AP). After washing with 0.1% TBST, the membrane was incubated with a horseradish peroxidase (HRP)-conjugated secondary antibody (dilution 1:1000) (Cell Signaling Technology) for 60 minutes at room temperature. The blot was developed using an enhanced chemiluminescence (ECL) solution to produce a chemiluminescence signal. For quantification, the density of protein bands on the western blot image, which was acquired using the peqlab gel documentation system (VWR International), was assessed by Image J. The final quantification reflects the relative amounts of protein as a ratio of each target protein band to the respective housekeeping protein.

4.4 | Immunohistochemistry

DU-145 cells were grown as monolayer culture on gelatine-coated cover slips. Sub-confluent cells were fixed for 20 minutes in ice-cold

methanol, and permeabilized in 1% Triton-X-100, diluted in phosphate buffered saline (PBST). Blocking against unspecific binding was performed by incubation for 1 hour in PBS, supplemented with 10% fat-free milk powder. Staining with a rabbit anti-human antibody against the autophagy marker LC3 (Proteintech, Cat. No. 14600-1-AP) (dilution 1:100) was performed at 4°C overnight. As secondary antibody an Alexa 488 anti-rabbit antibody was used. Cell nuclei were stained by the nuclear marker DRAQ5 (Thermo Fisher Scientific). In each experiment 20 cells were assessed. Immunohistochemical analysis was performed by use of a confocal laser scanning microscope (Leica SP2 AOBS) using the 488 nm line of an argon ion laser for Alexa 488 excitation and a 633 nm line of a He/Ne laser from DRAQ5 excitation.

4.5 | Drug extrusion assay

Multicellular tumour spheroids (10-day-old) were loaded for 20 minutes with the live cell indicator calcein AM (0.1 μ M) (Thermo Fisher) or pheophorbide A (5 μ mol/L) (Cayman Chemical) for 60 minutes, either in absence or upon pre-incubation with 40 nmol/L FK866 (calcein), or 20 nmol/L FK866 (pheophorbide A) for 24 hours. Subsequently, tumour spheroids were washed with fresh cell culture medium and cellular calcein fluorescence was monitored at 0, 60, 120 and 180 minutes using the 488 nm argon laser band of a confocal microscope (Leica SP2 AOBS; Leica Microsystems) and emission at 515–525 nm. Pheophorbide A was excited using the 633-nm HeNe laser of the confocal setup and fluorescence emission was analyzed with a 660-nm bandpass filter. Pheophorbide A efflux was assessed every 60 seconds for 45 minutes.

4.6 | Cell motility assay

Ten-day-old DU-145 tumour spheroids were plated on 6-cm tissue culture plates, which resulted in attachment and outgrowth of tumour cells from the spheroid core. For visualization, outgrown tumour spheroids were stained with 0.1 μ mol/L calcein AM. The outgrowth area was set into relation to the diameter of spheroid core as an indication of tumour cell motility.

4.7 | Cell toxicity assay

DU-145 cancer cells grown as multicellular tumour spheroids were treated from day 10 to day 15 of cell culture with FK866. Subsequently, cell culture medium was removed and tumour spheroids were double-labelled in PBS with the cell toxicity marker Sytox

green which labels dead cells (Thermo Fisher) (0.1 μ M) and DRAQ5 (Abcam) (1 μ mol/L) which labels live and dead cells for 15 minutes at room temperature. Finally tumour spheroids were washed with fresh cell culture medium and analyzed by confocal microscopy. Excitation of Sytox green was performed using the argon laser of the confocal microscope at 488 nm, and emission was recorded at 515–525 nm. DRAQ5 was excited with a He/Neon laser at 633 nm and emission recorded at >655 nm.

4.8 | Determination of intracellular ATP

The ATP content of tumour spheroids was determined by use of a fluorometric ATP assay kit (Sigma-Aldrich, Cat. No. ab83355), which is based on the phosphorylation of glycerol in order to generate a product that can be quantified fluorometrically (Ex/Em = 535/587 nm). Briefly, 10-day-old tumour spheroids were treated for 48 hours with either 20 or 40 nmol/L FK866 or vehicle. Subsequently, they were homogenized by addition of ATP assay buffer and centrifuged at 13 000 g. ATP was determined in the supernatant as described by the provider by use of a microplate reader (Tecan Infinite 200, Thermo Fisher), and ATP concentrations were calculated from a calibration curve which was determined before the experiment.

4.9 | Statistical analysis

For statistical analysis GraphPad InStat statistics software (GraphPad Software Inc., La Jolla, CA, USA) was used. Data are given as mean values \pm standard error of the mean (SEM), with n denoting the number of experiments performed with independent cell cultures. In each experiment at least 20 multicellular tumour spheroids were analyzed unless otherwise indicated. Student's *t* test for unpaired data and one-way ANOVA with Dunnett's post hoc test were applied as appropriate for statistical analysis. A value of *P* \leq .05 was considered significant.

CONFLICT OF INTEREST

The authors have no conflict of interest regarding this work.

AUTHOR CONTRIBUTIONS

The contribution of the authors was as follows: HS experimental work, manuscript preparation; FS experimental work; HK experimental work; FK experimental work, MW conceptualization. All authors agreed with the content of this manuscript.

PEER REVIEW

The peer review history for this article is available at <https://publons.com/publon/10.1111/1440-1681.13452>.

DATA AVAILABILITY STATEMENT

The data that support the findings of this study are available from the corresponding author, [HS], upon reasonable request.

ORCID

Heinrich Sauer  <https://orcid.org/0000-0002-9144-4728>

REFERENCES

- Bose S, Le A. Glucose metabolism in cancer. *Adv Exp Med Biol*. 2018;1063:3-12.
- Ward PS, Thompson CB. Metabolic reprogramming: a cancer hallmark even warburg did not anticipate. *Cancer Cell*. 2012;21(3):297-308.
- Sampath D, Zabka TS, Misner DL, O'Brien T, Dragovich PS. Inhibition of nicotinamide phosphoribosyltransferase (NAMPT) as a therapeutic strategy in cancer. *Pharmacol Ther*. 2015;151:16-31.
- Shoba B, Lwin ZM, Ling LS, Bay BH, Yip GW, Kumar SD. Function of sirtuins in biological tissues. *Anat Rec (Hoboken)*. 2009;292(4):536-543.
- Hara N, Yamada K, Shibata T, Osago H, Hashimoto T, Tsuchiya M. Elevation of cellular NAD levels by nicotinic acid and involvement of nicotinic acid phosphoribosyltransferase in human cells. *J Biol Chem*. 2007;282(34):24574-24582.
- Chowdhry S, Zanca C, Rajkumar U, et al. NAD metabolic dependency in cancer is shaped by gene amplification and enhancer remodelling. *Nature*. 2019;569(7757):570-575.
- Wang B, Hasan MK, Alvarado E, Yuan H, Wu H, Chen WY. NAMPT overexpression in prostate cancer and its contribution to tumor cell survival and stress response. *Oncogene*. 2011;30(8):907-921.
- Yaku K, Okabe K, Hikosaka K, Nakagawa T. NAD metabolism in cancer therapeutics. *Front Oncol*. 2018;8:622.
- Lucas S, Soave C, Nabil G, et al. Pharmacological inhibitors of NAD biosynthesis as potential anticancer agents. *Recent Pat Anticancer Drug Discov*. 2017;12(3):190-207.
- Galli U, Colombo G, Travelli C, Tron GC, Genazzani AA, Grolla AA. Recent advances in NAMPT inhibitors: a novel immunotherapeutic strategy. *Front Pharmacol*. 2020;11:656.
- Aguilar-Gallardo C, Simon C. Cells, stem cells, and cancer stem cells. *Semin Reprod Med*. 2013;31(1):5-13.
- Peiris-Pages M, Martinez-Outschoorn UE, Pestell RG, Sotgia F, Lisanti MP. Cancer stem cell metabolism. *Breast Cancer Res*. 2016;18(1):55.
- Mamun MA, Mannoor K, Cao J, Qadri F, Song X. SOX2 in cancer stemness: tumor malignancy and therapeutic potentials. *J Mol Cell Biol*. 2020;12(2):85-98.
- Souza AG, Silva IBB, Campos-Fernandez E, et al. Comparative assay of 2D and 3D cell culture models: proliferation, gene expression and anticancer drug response. *Curr Pharm Des*. 2018;24(15):1689-1694.
- Wartenberg M, Frey C, Diederhagen H, Ritgen J, Hescheler J, Sauer H. Development of an intrinsic P-glycoprotein-mediated doxorubicin resistance in quiescent cell layers of large, multicellular prostate tumor spheroids. *Int J Cancer*. 1998;75(6):855-863.
- He M, Wu H, Jiang Q, et al. Hypoxia-inducible factor-2alpha directly promotes BCRP expression and mediates the resistance of ovarian cancer stem cells to adriamycin. *Mol Oncol*. 2019;13(2):403-421.
- Min L, Chen Q, He S, Liu S, Ma Y. Hypoxia-induced increases in A549/CDDP cell drug resistance are reversed by RNA interference of HIF-1alpha expression. *Mol Med Rep*. 2012;5(1):228-232.
- Ma Y, Liang D, Liu J, et al. Prostate cancer cell lines under hypoxia exhibit greater stem-like properties. *PLoS One*. 2011;6(12):e29170.
- Mansour M, van Ginkel S, Dennis JC, et al. The combination of Omega-3 stearidonic acid and docetaxel enhances cell death over docetaxel alone in human prostate cancer cells. *J Cancer*. 2018;9(23):4536-4546.
- Doublier S, Belisario DC, Polimeni M, et al. HIF-1 activation induces doxorubicin resistance in MCF7 3-D spheroids via P-glycoprotein expression: a potential model of the chemo-resistance of invasive micropapillary carcinoma of the breast. *BMC Cancer*. 2012;12:4.

21. Tiberghien F, Loo F. Ranking of P-glycoprotein substrates and inhibitors by a calcein-AM fluorometry screening assay. *Anticancer Drugs*. 1996;7(5):568-578.
22. Silbermann K, Shah CP, Sahu NU, et al. Novel chalcone and flavone derivatives as selective and dual inhibitors of the transport proteins ABCB1 and ABCG2. *Eur J Med Chem*. 2019;164:193-213.
23. Portillo-Lara R, Alvarez MM. Enrichment of the cancer stem phenotype in sphere cultures of prostate cancer cell lines occurs through activation of developmental pathways mediated by the transcriptional regulator DeltaNp63alpha. *PLoS One*. 2015;10(6):e0130118.
24. Tan B, Young DA, Lu ZH, et al. Pharmacological inhibition of nicotinamide phosphoribosyltransferase (NAMPT), an enzyme essential for NAD⁺ biosynthesis, in human cancer cells: metabolic basis and potential clinical implications. *J Biol Chem*. 2013;288(5):3500-3511.
25. Kristensen AR, Schandorff S, Hoyer-Hansen M, et al. Ordered organelle degradation during starvation-induced autophagy. *Mol Cell Proteomics*. 2008;7(12):2419-2428.
26. Cea M, Cagnetta A, Patrone F, Nencioni A, Gobbi M, Anderson KC. Intracellular NAD⁺ depletion induces autophagic death in multiple myeloma cells. *Autophagy*. 2013;9(3):410-412.
27. Kozako T, Aikawa A, Ohsugi T, et al. High expression of NAMPT in adult T-cell leukemia/lymphoma and anti-tumor activity of a NAMPT inhibitor. *Eur J Pharmacol*. 2019;865:e172738.
28. Huang KM, Hu S, Sparreboom A. Drug transporters and anthracycline-induced cardiotoxicity. *Pharmacogenomics*. 2018;19(11):883-888.
29. Wartenberg M, Richter M, Datchev A, et al. Glycolytic pyruvate regulates P-Glycoprotein expression in multicellular tumor spheroids via modulation of the intracellular redox state. *J Cell Biochem*. 2010;109(2):434-446.
30. Emmanouilidi A, Casari I, Gokcen Akkaya B, et al. Inhibition of the lysophosphatidylinositol transporter ABCC1 reduces prostate cancer cell growth and sensitizes to chemotherapy. *Cancers (Basel)*. 2020;12(8):2022.
31. Strouse JJ, Ivnitski-Steele I, Waller A, et al. Fluorescent substrates for flow cytometric evaluation of efflux inhibition in ABCB1, ABCC1, and ABCG2 transporters. *Anal Biochem*. 2013;437(1):77-87.
32. Robey RW, Steadman K, Polgar O, et al. Pheophorbide a is a specific probe for ABCG2 function and inhibition. *Cancer Res*. 2004;64(4):1242-1246.
33. Briz O, Perez-Silva L, Al-Abdulla R, et al. What "The Cancer Genome Atlas" database tells us about the role of ATP-binding cassette (ABC) proteins in chemoresistance to anticancer drugs. *Expert Opin Drug Metab Toxicol*. 2019;15(7):577-593.
34. Nagaya M, Hara H, Kamiya T, Adachi T. Inhibition of NAMPT markedly enhances plasma-activated medium-induced cell death in human breast cancer MDA-MB-231 cells. *Arch Biochem Biophys*. 2019;676:e108155.
35. Sociali G, Raffaghello L, Magnone M, et al. Antitumor effect of combined NAMPT and CD73 inhibition in an ovarian cancer model. *Oncotarget*. 2016;7(3):2968-2984.
36. Sanokawa-Akakura R, Ostrakhovitch EA, Akakura S, Goodwin S, Tabibzadeh S. A H2S-Nampt dependent energetic circuit is critical to survival and cytoprotection from damage in cancer cells. *PLoS One*. 2014;9(9):e108537.
37. Lucena-Cacace A, Otero-Albiol D, Jimenez-Garcia MP, Peinado-Serrano J, Carnero A. NAMPT overexpression induces cancer stemness and defines a novel tumor signature for glioma prognosis. *Oncotarget*. 2017;8(59):99514-99530.
38. Lucena-Cacace A, Umeda M, Navas LE, Carnero A. NAMPT as a de-differentiation-inducer gene: NAD⁺ as core axis for Glioma cancer stem-like cells maintenance. *Front Oncol*. 2019;9:292.
39. Yamamoto M, Suzuki S, Togashi K, et al. AS602801 sensitizes ovarian cancer stem cells to paclitaxel by down-regulating MDR1. *Anticancer Res*. 2019;39(2):609-617.
40. Li S, Zhao Q, Wang B, Yuan S, Wang X, Li K. Quercetin reversed MDR in breast cancer cells through down-regulating P-gp expression and eliminating cancer stem cells mediated by YB-1 nuclear translocation. *Phytother Res*. 2018;32(8):1530-1536.
41. Kawai N, Hirohashi Y, Ebihara Y, et al. ABCG2 expression is related to low 5-ALA photodynamic diagnosis (PDD) efficacy and cancer stem cell phenotype, and suppression of ABCG2 improves the efficacy of PDD. *PLoS One*. 2019;14(5):e0216503.
42. Salaroglio IC, Gazzano E, Kopecka J, et al. New tetrahydroisoquinoline derivatives overcome Pgp activity in brain-blood barrier and Glioblastoma Multiforme in vitro. *Molecules*. 2018;23(6):1401.
43. Sharif T, Martell E, Dai C, et al. Autophagic homeostasis is required for the pluripotency of cancer stem cells. *Autophagy*. 2017;13(2):264-284.
44. Olesen UH, Thougard AV, Jensen PB, Sehested M. A preclinical study on the rescue of normal tissue by nicotinic acid in high-dose treatment with APO866, a specific nicotinamide phosphoribosyltransferase inhibitor. *Mol Cancer Ther*. 2010;9(6):1609-1617.
45. O'Brien T, Oeh J, Xiao Y, et al. Supplementation of nicotinic acid with NAMPT inhibitors results in loss of in vivo efficacy in NAPRT1-deficient tumor models. *Neoplasia*. 2013;15(12):1314-1329.

How to cite this article: Sauer H, Kampmann H, Khosravi F, Sharifpanah F, Wartenberg M. The nicotinamide phosphoribosyltransferase antagonist FK866 inhibits growth of prostate tumour spheroids and increases doxorubicin retention without changes in drug transporter and cancer stem cell protein expression. *Clin Exp Pharmacol Physiol*. 2021;48:422-434. <https://doi.org/10.1111/1440-1681.13452>